Journal of Controlled Release 146 (2010) 212–218

Contents lists available at ScienceDirect

Journal of Controlled Release

journal homepage: www.elsevier.com/locate/jconrel

Localized doxorubicin chemotherapy with a biopolymeric nanocarrier improves survival and reduces toxicity in xenografts of human breast cancer

Shuang Cai [a], Sharadvi Thati [a], Taryn R. Bagby [a], Hassam-Mustafa Diab [a], Neal M. Davies [b], Mark S. Cohen [c], M. Laird Forrest [a,*]

[a] Department of Pharmaceutical Chemistry, University of Kansas, United States
[b] Department of Pharmaceutical Sciences, Washington State University, United States
[c] Department of Surgery, University of Kansas Medical Center, United States

ARTICLE INFO

Article history:
Received 2 December 2009
Accepted 5 April 2010
Available online 18 April 2010

Keywords:
Polymeric drug carrier
Localized chemotherapy
Doxorubicin
Breast cancer
Localized chemotherapy

ABSTRACT

Patients with metastatic breast cancer have a five-year survival rate of 27% compared to 98% for localized cancer, and the presence of even a few cancer cells in lymph nodes, known as isolated tumor cells or nanometastases, significantly increases the risk of relapse in the absence of aggressive treatment. Therefore, diagnosis and treatment of lymphatic metastases in early breast cancer plays an important role in patient survival. Here, we demonstrate the first description of a delivery system for localized doxorubicin chemotherapy to the breast tissue. The hyaluronan–doxorubicin nanoconjugate exhibits a sustained release characteristic *in vitro* and *in vivo* in the breast tissues of rodents bearing human breast cancer xenografts. In addition, the conjugate reduces dose-limiting cardiac toxicity with minimal toxicity observed in normal tissues. Finally, the conjugate dramatically inhibits breast cancer progression *in vivo*, leading to an increased survival rate. Thus, localized chemotherapy to the breast lymphatics with a nanocarrier may represent an improved strategy for treatment of early stage breast cancers.

1. Introduction

Doxorubicin (DOX) is among the most effective chemotherapeutics used for the treatment of cancers including breast, ovarian, sarcomas, pediatric solid tumors, Hodgkin's disease, multiple myeloma, and non-Hodgkin's lymphomas. Despite the success of DOX against many cancers, its use can be severely limited by its cardiac toxicity including development of a cardiomyopathy, often refractory to common medications, which can progress to biventricular failure and even death (reviewed in Takemura and Fujiwara [1]). Technologies such as polymeric micelles [2], synthetic polymer conjugates [3], and antibody targeted carriers [4] have demonstrated reduced or altered toxicity in Phase I trials, yet the therapeutic efficacy of these formulations has yet to be demonstrated. In the absence of safer, efficacious systemic formulations, localized delivery of DOX may improve tolerability and improve efficacy, especially in the treatment of early breast cancer.

Early breast cancers will typically spread initially from the primary tumor site to regional lymph nodes in the axilla prior to systemic dissemination. Surgery and radiation therapy can be effective, but result in significant side effects including painful lymphedema [5]. There is debate over the risk vs the benefit of aggressive therapy for patients with isolated tumor cells or nanometastases in the axillary lymph nodes; however, recent studies support that there is a strong risk factor for metastatic relapse in patients with nodal nanometastases, with occult lymph node disease accounting for up to 50% of metastatic recurrences [6] and a hazard ratio of 1.5 for patients with isolated cancer cells who do not receive adjuvant systemic chemotherapy [7]. We therefore sought to develop a formulation of DOX that could be given locally and concentrated to the draining lymphatic basin of the breast, where early metastases are more prevalent, while sparing normal tissues from many of the organ toxicities associated with systemic chemotherapy. DOX is a potent vesicant, so direct s.c. injection (leading to lymphatic drainage) is not viable; however, conjugates of DOX and a lymphatically targeted carrier may avoid severe tissue toxicity through improved localization to the lymphatic basin. For this purpose, hyaluronan may be an ideal carrier.

Hyaluronan (HA) is a polysaccharide, of alternating D-glucuronic acid and *N*-acetyl D-glucosamine, found in the connective tissues of the body and cleared primarily by the lymphatic system (12 to 72 h turnover half-life [8]). After entering the lymphatic vessel, HA is transported to nodes where it is catabolized by receptor-mediated endocytosis and lysosomal degradation. Several studies have correlated increased HA synthesis and uptake with cancer progression and metastatic potential [9,10]. Breast cancer cells are known to have greater uptake of HA than normal tissues [11], requiring HA for

Abbreviations: AUC, area-under-the-curve; CDDP, *cis*-diamminedichloroplatinum (II), cisplatin; C_{max}, peak measured concentration of drug; HA, hyaluronan; HA–DOX, Hyaluronan–doxorubicin conjugate.

* Corresponding author. Tel.: +1 785 864 4388; fax: +1 785 864 5736.
E-mail address: mforrest@ku.edu (M.L. Forrest).

0168-3659/$ – see front matter © 2010 Elsevier B.V. All rights reserved.
doi:10.1016/j.jconrel.2010.04.006

high P-glycoprotein expression, the primary contributor to DOX resistance [12]. Knockout of HA receptors has been reported to prevent migration of cancers that initially spread intralymphatically [13]. Furthermore, invasive breast cancer cells overexpress CD44, the primary receptor for HA [14], and are dependent on high concentrations of CD44-internalized HA for proliferation (reviewed in Gotte and Yip [11]). Doxorubicin conjugates to HA may represent a natural lymphatic and breast cancer-targeted delivery platform to improve efficacy against lymphatic metastases.

Several HA–DOX conjugates have been reported which used non-reversible or peptide linkers and had a considerable loss of anticancer activity [15–17]. We report herein a new pH-sensitive, reversible hydrazone HA–DOX conjugate with potent anticancer activity against breast cancer cells *in vitro* demonstrating excellent cell uptake and retention. Furthermore, we show that HA is drained to the axilla basin of rats after s.c. injection into the mammary fat pad, laying the foundation for future studies of pharmacokinetics, and anti-tumor activity in rodent models.

2. Materials and methods

2.1. Materials

Hyaluronan from microbial fermentation was purchased from Lifecore Biomedical (Chaska, MN) as sodium hyaluronate and used without further purification. All other reagents were purchased from Sigma Chemical Co. (St. Louis, MO) or Thermo Fisher Scientific (Waltham, MA) and were of ACS grade or better. Milli-Q water was used in all experiments. Cell lines were obtained from American Type Culture Collection (ATCC, Manassas, VA) and were maintained according to ATCC recommendations. Caution: doxorubicin is extremely toxic and all chemical waste (including dialysis baths) was treated as hazardous waste and disposed of accordingly.

2.2. Synthesis of HA–DOX conjugates

Direct conjugation of drugs to HA is inefficient due to the steric hindrance of the polysaccaride backbone and low reactivity of the carboxylate group. HA was derivatized with adipic acid dihydrazide (ADH), according to the procedure of Luo et al. [18]. Briefly, HA (200 mg, 35 kDa) was dissolved in 40 mL ddH_2O with ADH (436 mg) and 1-ethyl-3-[3-(dimethylamino)-propyl]carbodiimide (EDCI, 48 mg). The solution pH was adjusted to 4.75 with 1 N HCl, and checked again after 10 min. The reaction was quenched by addition of 0.1 N NaOH to pH 7.0 (Fig. 1). The resulting solutions were dialyzed against ddH_2O for two days with bath changes every 12 h. After dialysis, the product was filtered (0.2 μm PS membrane, Millipore), and lyophilized. The degree of substitution was determined to be 33% by ^{1}H NMR in D_2O using the ratio of ADH methylene protons to HA acetyl methyl protons.

Conjugation of DOX to HA was accomplished by formation of a hydrazone between the ketone of DOX and the hydrazide side chain of HA–ADH [19]. HA–ADH (110 mg) was dissolved in 30 mL of 2 mM sodium phosphate buffer (pH 6.5). DOX·HCl (2 mL, 2 mg/mL) was added dropwise in 25 mL of H_2O. The solution was adjusted to pH 6.5 with 0.1 N NaOH and after 2 h was dialyzed against 2 mM sodium phosphate buffer (pH 7.8), with twice daily changes until no further color change was observed (2 days). Solutions were protected from light at all times. The degree of conjugation was determined by UV/Vis spectrophotometry at 480 nm using a standard calibration curve (1–100 μg/mL). Conjugation was confirmed by equivalent elution times using gel permeation chromatography (GPC; Shodex HQ-806 M column, 0.8 mL/min 20 mM HEPES, pH 7.2) with refractive index and fluorescent detection (ex/em 480/590 nm).

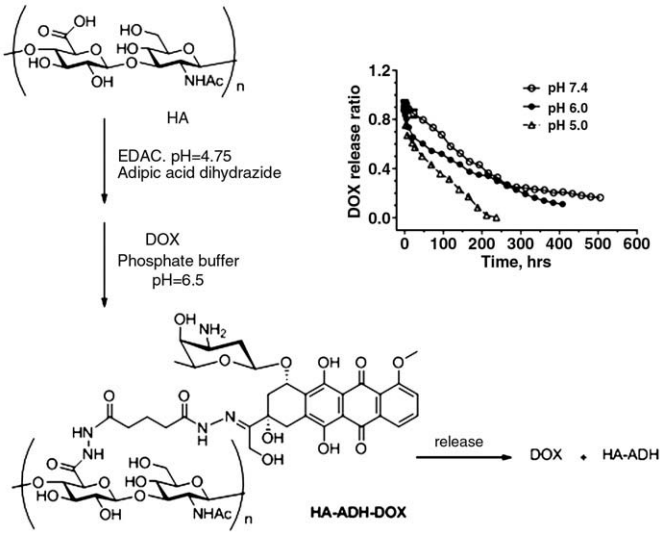

Fig. 1. Synthesis of hyaluronan–doxorubicin (HA–DOX) conjugate (left panel). *In vitro* release of DOX from HA–DOX at pH 5.0, 6.0 and 7.4 (right panel).

2.3. In vitro drug release

HA–DOX was dissolved in PBS adjusted to 5.0, 6.0 or 7.4 and sealed in dialysis tubing (10,000 MWCO). The dialysis tubings were placed in PBS bath at pH 5.0, 6.0 or 7.4, and 100 μL aliquots from the bags were analyzed by GPC with coupled refractive index and fluorescent (ex/em 480/590) detectors. The PBS solution was changed 5–10 times daily and the ratio of the peak areas of HA to DOX was calculated for up to approximately 500 h.

2.4. Cell toxicity and uptake

Cell lines were seeded into 12-well plates (50,000 cells/well) containing a poly-L-lysine coated coverslip (Fisher Scientific). After 24 h, DOX, HA-DOX, or HA was applied, and after 6 h, the media was refreshed. After 12 h, cells were examined by fluorescent microscopy (ex/em 480/590). Images were adjusted for contrast and brightness with no further manipulation. Cell growth inhibition was determined in 96-well plates (3000 cells/well in 100 μL) ($n=3$, 12 wells/concentration). The drug or conjugate in PBS was applied after 24 h, and 72 h post-addition, resazurin blue in 10 μL PBS was applied to each well (final 5 mM). After 4 h, well fluorescence was measured (ex/em 560/590) (SpectraMax Gemini, Molecular Devices), and the IC_{50} concentration determined as the midpoint between saline (positive) and cell-free (negative) controls.

2.5. Pharmacokinetics

Sprague–Dawley rats (200–300 g females, Charles Rivers) were placed under isoflurane anesthesia and cannulated at the jugular veins. Animals were allowed to recover with access to food and water overnight. Then they were injected s.c. (100 μL) into the left mammary fat pad with HA-DOX (4 mg/kg DOX·HCl equivalent), or i.v. into the jugular vein with 2 mg/mL DOX·HCl in 0.9% saline ($n=4$). Blood was sampled from the jugular vein (200–300 μL) at 0 min, 5 min, 30 min, 1 h, 2 h, 4 h, 6 h, 12 h and 24 h. Plasma was separated by centrifugation from whole blood and stored at −80 °C freezer until analysis. At 24 h, the animals were euthanized by isoflurane overdose.

The pharmacokinetic parameters were determined using SAAM II Version 1.2 software. A two-compartmental model was utilized for both i.v. (DOX) and s.c. (HA–DOX) data. Pharmacokinetic data were collected from 0 to 24 h and were analyzed, resulting in a series of biexponential plasma level-time curves. Pharmacokinetic parameters

such as volume of distribution, clearance, area-under-the-curve, mean residence time and elimination half time were determined as reported in Table 1.

2.6. Toxicology

2.6.1. Renal toxicity of DOX and HA–DOX

The potential renal toxicity of DOX and HA–DOX was determined using lysosomal enzyme, β-N-acetylglucosaminidase (NAG) (Sigma), which acts as an indicator of ongoing kidney damage. Two groups ($n=3$) of Sprague–Dawley rats were treated with 4 mg/kg of DOX i.v. or HA–DOX s.c., respectively. Animals were housed in metabolic cages and their urine was collected daily. The urine samples were centrifuged and stored at −80 °C freezer until analysis. The animals were euthanized after 8–10 days. The urine samples were analyzed for the concentration of NAG upon hydrolyzing the NAG substrate, 4-nitrophenyl.

2.6.2. Cardiac toxicity of DOX and HA–DOX

The cardiac toxicity of DOX and HA–DOX was determined using a rat cardiac Troponin-I (cTnI) ELISA kit (Life Diagnostic). Sprague–Dawley rats were cannulated in the jugular vein and injected with 4 mg/kg DOX·HCl solution i.v. or HA–DOX s.c. into the mammary fat pad. Blood samples were collected at 0, 8, 16, 24 h and 2, 3, 4, 5 and 6 days from the jugular vein and centrifuged to obtain the plasma. Samples were stored at −80 °C freezer until analysis.

2.7. Pathology

2.7.1. DOX s.c. vs HA–DOX s.c.

Sprague–Dawley rats were divided into two groups and treated with DOX s.c. or HA–DOX s.c. ($n=6$/group) at either 2 or 4 mg/kg. Three rats from each group were euthanized 6 h after drug administration and the other three were euthanized 24 h after drug administration. The liver, bilateral kidneys, spleen, lungs, heart, right (ipsilateral) and left (contralateral) axillary nodes, and brain were excised intact and stored in 80% alcoholic formalin solution overnight for fixation before slide mounting. Mounting using haematoxylin & eosin (H&E) staining was conducted by Veterinary Lab Resources (Kansas City, KS). The pathological examination was performed by a blinded board-certified veterinarian pathologist (University of Kansas Medical Center, Kansas City, KS).

2.7.2. Tumor model and in vivo release of doxorubicin

MDA-MB-468LN human breast cancer cells (kind gift of Ann Chambers, London University) were implanted into the mammary fat pad of female nude mice from a small incision using a 27-ga needle (100 μL, 10^6 cells) under pentobarbital sedation. The incision was closed using sterilized staples, which were removed when the incision was healed. Tumor growth was monitored by CSI Maestro imaging system and tumor size was measured twice a week by a digital caliper on mice anesthetized with 1.5–2% isoflurane in 50% oxygen-50% ambient air mixture. Tumor volume was calculated using equation: tumor volume (mm^3) $=0.52\times(\text{width})^2\times\text{length}$.

The MDA-MB-468LN human breast cancer cell line can be transfected with a GFP–neomycin expression vector and selected with G418 to express green fluorescent protein (GFP) so metastasis can be monitored by whole animal imaging. For example, nude mice with mammary tumors (approximately 500 mm^3) were injected peritumorally with a single dose of 3.5 mg/kg HA–DOX solution. Images of the primary tumor and lymphatic metastases were captured from day 1 to day 9 after drug administration. Distribution characteristics of HA–DOX were monitored and percentage release calculated by spectrally unmixing tumor GFP, DOX, and skin auto-fluorescence using the Maestro software.

2.7.3. Treatment

Nude mice were injected into the first mammary fat pad on the right side with 10^7 MDA-MB-468LN cells and randomly divided into four groups including saline, HA, DOX and HA–DOX ($n=5$/group). Animals of the saline and HA control groups were euthanized once their tumor size reached 2000 mm^3. Animals of DOX or HA–DOX treatment groups were euthanized once their tumor reached 1000 mm^3 in size or 24 weeks after tumor cells were injected. In addition, animals were euthanized during the study if tumors ulcerated or the animals acquired opportunistic infections. Mammary tumors were observed at the 3rd week after tumor cells were implanted. All treatments were administered at the 3rd and 4th week after tumor cells implantation. Two doses of 3.5 mg/kg DOX or physiological saline were administered i.v. via tail vein; whereas two doses of 3.5 mg/kg of HA–DOX or HA was administered s.c. 2–3 mm from the tumor margins (see white arrows in Fig. 4). The size of the primary tumors was measured weekly.

Table 1
The pharmacokinetic data were fitted using a two-compartmental model. Data are shown as means and standard deviation. *Study groups, i.v. DOX and s.c. HA–DOX, differed significantly for MRT(syst) and $C_{max}(t)$. Significance defined as $p<0.05$ using Student t-test ($n=4$).

Parameters	Unit	DOX (i.v.)	HA–DOX (s.c.)
Vol	L/kg	0.430 ± 0.272	0.096 ± 0.084
A	μg/mL	4.415 ± 1.515	30.974 ± 29.980
B	μg/mL	0.078 ± 0.013	0.086 ± 0.012
$AUC_{0-24\,h}$	(μg h)/mL	2.061 ± 0.824	2.201 ± 0.905
Cl	L/(kg h)	1.283 ± 0.404	1.261 ± 0.564
MRT (syst)	h	8.247 ± 4.944*	26.501 ± 10.703*
$t_{1/2}(\beta)$	h	0.226 ± 0.072	0.199 ± 0.293
$C_{max}(t)$	μg/mL (min)	2.580 ± 0.670 (5)*	0.130 ± 0.020 (30)*

3. Results

3.1. HA–DOX conjugation

Conjugation of DOX and HA–ADH were verified by equivalent retention times using gel permeation chromatography coupled with refractive index (green) and fluorescent detection (blue) (480/590 nm). The HA (green) and bound DOX (blue) were both eluted at approximately 11 min. A series of concentrations of DOX standard solution was prepared to generate a calibration curve. The concentration of the standard solution were 1, 2, 5, 10, 25, 50 and 100 μg/mL ($R^2=0.99$). Absorbance at 450 nm was measured and it was due to the UV absorbance of DOX. HA does not exhibit UV absorbance (data not shown). Specifically, the loading degree was calculated to be 5.2% (wt/wt). In general, the optimal loading degree of DOX was maintained to be in a range of 5–15% (wt/wt) to obtain the maximum solubility and the least volume of solution administered in animal studies.

3.2. In vitro drug release

The release half-life of DOX was determined to be 172 h at pH 7.4, 110 h at pH 6.0 and 45 h at pH 5.0 (Fig. 1). The shorter half-life at pH 5.0 was due to the faster hydrolysis of the hydrazone between the ketone of DOX and hydrazide of ADH. The extended half-life at physiological pH was consistent with the sustained release characteristics of HA–DOX conjugates.

3.3. Cell toxicity and uptake

Both free DOX and HA–DOX conjugate were taken up by MDA-MB-231 cells after 6 h incubation (data not shown). In addition, HA–DOX conjugates exhibit slightly lower toxicities than free doxorubicin in

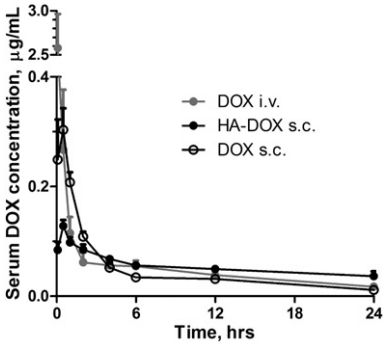

Fig. 2. Serum DOX concentration-time curves.

cell culture: MDA-MB-468LN, 221 and 515 nM (DOX and HA–DOX, respectively); MDA-MB-231, 147 and 588 nM; and MCF-7, 221 and 1287 nM. However, the conjugate remains potent for all the breast cancer cell lines tested with IC_{50} values in the nanomolar range. HA exhibits no toxicity to human cells over the concentration range examined (up to 10 mg/mL, data not shown).

3.4. Pharmacokinetics

The pharmacokinetics of s.c. HA–DOX were compared to i.v. DOX and s.c. DOX in Sprague–Dawley rats. The peak plasma concentration of i.v. DOX was 18.8-fold greater than s.c. HA–DOX (Fig. 2). The release of DOX into the systemic circulation was slow, and the resulting plasma AUC of HA–DOX did not exhibit significant difference from i.v. therapy. The peak plasma concentration of s.c. DOX was 1.3 greater than s.c. HA–DOX and the AUC of s.c. DOX was slightly lower than s.c. HA–DOX. The serum DOX level measured in HA–DOX was associated with the free unbound drug instead of the sum of free drug and HA bound drug due to the difficulty cleaving DOX from the polymer backbone in serum samples. Thus, the actual total DOX level in the serum would be expected to be higher for s.c. HA–DOX, resulting in a greater AUC.

A two-compartment model was selected to describe the biexponential nature of the pharmacokinetics of HA–DOX and DOX. The predicted volume of distribution of DOX was determined to be approximately 3.4-fold greater than HA–DOX. In addition, both routes of drug administration resulted in similar values of area-under-the-curve ($AUC_{0-24\ h}$), clearance and elimination half-life. However, s.c. HA–DOX exhibited a 2.2-fold increase in systemic mean residence time, which is consistent with the sustained release nature of the polymer drug conjugate. Finally, the observed peak plasma concentration of i.v. DOX is shown to be 18.8-fold higher than that of the s.c. HA–DOX, which may cause potential tissue toxicity, such as cardiac toxicity (dose-limiting) and hepatoxicity (the liver is the major organ of DOX metabolism) (Table 1).

3.5. Toxicology

3.5.1. Renal toxicity of DOX and HA–DOX

Renal toxicity of DOX and HA–DOX was evaluated using lysosomal enzyme, β-N-acetylglucosaminidase (NAG). NAG is a urinary enzyme that is sensitive to early renal tubular dysfunction. It is commonly and widely used as a biomarker for the early detection of renal tubular damage. NAG is expressed in normal kidney at a relatively constant level. However, raised urinary NAG activity in a chemotherapy treated animal may be associated with renal tubular dysfunction caused by the chemotherapeutic agent administered. NAG activity in s.c. HA–DOX treated animals exhibited a relatively steady level during the study period of 9 days. On the other hand, animals that were treated with i.v. DOX demonstrated a slight increase in NAG activity stating day 2 after drug administration. A dose of 4 mg/kg DOX or HA–DOX may not be sufficient to induce a significant renal tubular damage (data not shown).

3.5.2. Cardiac toxicity of DOX and HA–DOX

Cardiac toxicity is the dose-limiting factor of doxorubicin chemotherapy. Doxorubicin-induced cardiomyopathy and congestive heart failure was believed to be dose-dependent. Troponin-I is a cardio-specific protein that is released from injured myocytes. It is a highly sensitive and specific biomarker of cardiac damage. The cTnI levels were both below the detection limit of the commercial available cTnI assay kit, indicating 4 mg/kg was a relatively low dose for an animal model of doxorubicin-induced cardiac toxicity (data not shown).

3.5.3. Histology

At the conclusion of the 6 and 24 h toxicity study (2 mg/kg), animals were euthanized and a full pathological examination performed. Heart, kidney, liver, lymph nodes and underlying tissue of the injection site were normal with no microscopic changes for all study groups (data not shown).

In addition, long term toxicity (8–10 days) of DOX and HA–DOX at 4 mg/kg was evaluated. Livers and lymph nodes were normal with no microscopic changes for both study groups. Underlying tissue of the injection site was examined for s.c. HA–DOX treated animals and no microscopic changes were diagnosed. Mild degeneration in the kidney was detected for both groups, indicating by sparse pyknotic nuclei and mild inflammation (data not shown). In addition, 83% of animals ($n=6$) receiving 4 mg/kg i.v. DOX were observed with myocyte degeneration including myofiber necrosis and myocarditis. In contrast, none of the animals ($n=5$) receiving s.c. HA–DOX had cardiac damage. Overall, the pathology studies demonstrated that the HA–DOX conjugates demonstrated lower incidence of cardiac toxicity compared to the conventional intravenous DOX treatment (Fig. 3).

3.5.4. Tumor model and in vivo release of doxorubicin

In order for our nanocarriers to deliver anticancer drugs to nano- and micrometastases in the breast loco-regional lymphatics, carriers should drain from the breast area to the diseased lymph nodes. We injected HA–DOX conjugates to verify drainage into the diseased lymph nodes, which were indicated by the dashed circle in the following figures. Injection site and location of the primary tumor were also labeled on each figure. Drainage of HA–DOX to loco-regional lymphatics in the axilla was characterized after nearby s.c. needle injection of a nodal breast tumor. After 1 day, 10% of the initial HA–DOX was in the area of the tumor and 66% was in the area of the tumor lymphatics and local tissues. After a week, 4% of original dose

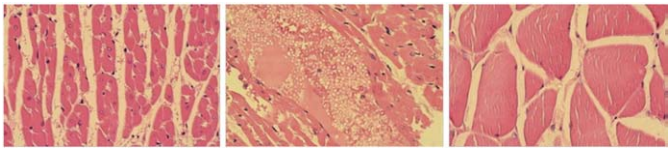

Fig. 3. Heart tissues of HA–DOX (left panel), DOX (middle panel) and underlying tissues of the HA–DOX injection site (right panel).

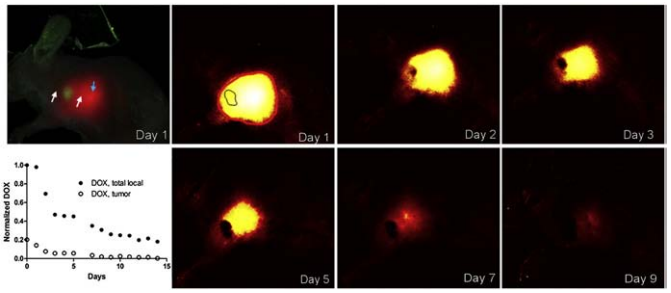

Fig. 4. Imaging of HA–DOX in the primary tumor and the surrounding lymphatics (day 1–9). HA–DOX was injected peritumorally (white arrows) with most of the carrier draining to the adjacent nodes (blue arrow). After spectrum unmixing and false coloring, the total DOX (within red circle) and tumoral DOX (within black circle) were integrated and normalized to day 0. Doxorubicin is false colored white–yellow–red with decreasing intensity.

remained in the primary tumor with 10% of the initial dose in the surrounding area and adjacent lymph nodes. Clearance of the drug from the tumor was 80% slower than from the surrounding tissues and lymphatics (Fig. 4). Intravenous DOX could not be detected in the tumor or surrounding tissues by *in vivo* imaging at any time point (data not shown).

3.5.5. Treatment

Animals treated with saline or HA had an average tumor size of approximately 2000 mm^3 in nine weeks, which indicated that HA does not alter the natural progression of breast cancer. On the other hand, the animals that were treated with three weekly doses of i.v. DOX developed a tumor with a size of 1000 mm^3 on average after approximately ten weeks. In contrast, animals in the s.c. HA–DOX treated group (three weekly equivalent doses of HA–DOX) reached an average tumor size of around 300 mm^3 ten weeks after the tumor cell injection (Fig. 5). In addition, 100% animal death occurred 18 weeks after the tumor cell injection for DOX treated group (Fig. 5). In contrast, 50% of HA–DOX treated animal lived through the study (24 weeks) with an average tumor delay of 4 weeks. Overall, the result of the tumor model suggests that HA–DOX conjugates achieved a higher anticancer efficacy relative to the conventional i.v. DOX therapy. HA–DOX conjugates delayed the tumor progression by approximately 10 weeks and increased the survival of the animals in relative to i.v. DOX treatment ($p<0.05$). We believe the carrier slowly released the active form of the drug, which subsequently drained to the adjacent axilla lymph nodes and the surrounding lymphatic regions.

4. Discussion

Doxorubicin is an anthracycline antibiotic that is widely used in cancer chemotherapy for the treatment of breast, ovarian, lung and bladder cancers. However, its dose-limiting toxicity severely limits its clinical use in patients, given its cumulative dose-dependent myocardial damage. This damage is caused by the generation of reactive oxidative species such as superoxide and hydrogen peroxide upon the reduction of doxorubicin to form an election deficient semiquinone. In addition, doxorubicin is an iron chelator, chelating Fe (III) and perturbing the transportation of iron into cells. It causes iron-deficient cell death of myocytes [20]. The purpose of this study is to investigate the feasibility of developing a doxorubicin bound conjugate using the FDA-approved biocompatible polymer hyaluronan, delivering doxorubicin to the loco-regional tissues and breast lymphatics. In addition, the polymer-DOX conjugate can lead to sustained release of the anticancer agent, resulting in lower peak plasma concentration, which may be associated with the dose-limiting cardiotoxicity of the drug.

Nanocarrier strategies for the delivery of drugs have been investigated extensively in the past decade. Among candidates of potential nanocarriers, hyaluronan represents a very promising substrate by being both a biocompatible and nonimmunogenic molecule. It has been used as a carrier for the delivery of a variety of chemotherapeutic agents, for instance, cisplatin [21], paclitaxel [22] and mitomycin C [23]. Strategies with different choices of spacers for the delivery of doxorubicin have been explored for optimal entrapment efficiency [24], specific tumor targeting [25] and higher cellular uptake [26]. A liposome-encapsulated formulation of doxorubicin (Doxil™) is currently available in human studies and promotes major benefits including reduced acute cardiotoxicity compared to i.v. DOX HCl and improved biodistribution [27]. However, liposomal DOX can cause palmar plantar erythrodysesthesia, a dermatologic toxic reaction associated with the leakage of a small amount of the drug from long-circulating liposomes into the cutaneous tissues of the palms and the soles of the feet [28]. A trial of DOX and liposomal DOX in 509 patients with metastatic breast cancer demonstrated reduced toxicity of liposomal DOX but no increase in survival [29]. In this study, we sought to develop controlled-release HA–DOX conjugates with reduced side effects compared to conventional DOX and liposomal DOX treatments with improved efficacy in locally advanced disease.

The nanoparticle conjugates were synthesized using a pH-sensitive linker, resulting in an adipic dihydrazide functionalized HA–DOX conjugates. The conjugate releases doxorubicin in a pH dependent fashion via a Schiff base mechanism, yielding free DOX and the polymer. The ratio of the release half lives of DOX from the polymer backbone at pH 5.0, 6.0 and 7.4 was determined to be approximately 1:2.4:3.8, clearly indicating a dependence of the

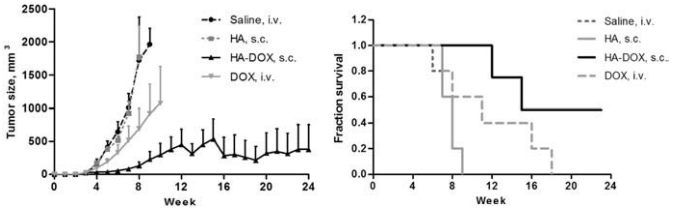

Fig. 5. Measurement of tumor size. Animals were administered saline, HA, equivalent doses of DOX and HA-DOX (3.5 mg/kg on DOX basis, n=5/group) (left panel). Survival curves of animals treated by DOX or HA-DOX. (n=5/group) (right panel).

hydrolysis of carbon–nitrogen double bond on pH changes. Thus, the carrier releases the active form of the drug more rapidly *in vivo* in an acidic environment as in the hypoxic environment within solid tumor masses, which may preferentially concentrate drug near the primary tumor or distant metastases of breast cancer cells, compared to a relatively neutral environment that surrounds normal cells.

Our previous study demonstrated that the intralymphatic delivery model using hyaluronan–cisplatin conjugate not only increases drug concentrations in loco-regional nodal tissues significantly compared to the standard cisplatin formulation, but it also exhibits sustained release kinetics, allowing lower peak plasma concentration which could translate into lower organ toxicity over time [21]. In this study, our intralymphatic delivery strategy was successfully applied to the HA–DOX delivery system, reducing the C_{max} by approximately 19-fold without compromising the plasma drug AUC. In addition, only the free DOX released from HA, as opposed to the sum of free and bound drug, was detected and analyzed for the calculation of the total drug AUC in the plasma. The actual total DOX concentration in the plasma may be higher, allowing a greater AUC compared to the standard DOX treatment. This may result in a lower dose of doxorubicin being required to achieve the same plasma and tissue drug level. HA–DOX injections therefore, could be considered for weekly or even biweekly injections, with great potential to replace daily conventional intravenous doxorubicin chemotherapy both from a standpoint of improved toxicity profiles, but also in terms of improvements in compliance and completion of chemotherapeutic regimens.

With regard to its pharmacokinetics, the difference in the volume of distribution in the plasma compartment, Vol, between i.v. DOX group and s.c. HA–DOX group was possibly due to the easier access to the surrounding tissues for free doxorubicin molecules as opposed to polymer bound DOX conjugates. Doxorubicin with a log *p* value of 1.3, pKa of 8.4, and a molecular weight of 544 g/mol, rapidly crosses lipid membrane and binds to tissues, resulting in a larger Vol [30]. Finally, HA–DOX conjugates exhibited a 2.2-fold increase in systemic mean residence time in relative to unbound DOX. The extended residence time of HA–DOX conjugates may decrease the frequency of doxorubicin chemotherapy and have potential to improve patient compliance and quality of life in a clinical setting. The sustained release drug-carrier model avoids peak and trough of plasma drug concentration in both drug distribution and elimination, leading to a well controlled drug level profile corresponding to its therapeutic index.

In spite of the high efficacy of DOX chemotherapy, its clinical use is limited due to its dose-limiting cardiac toxicity along with its renal toxicity and hepatoxicity. Tissue toxicities of doxorubicin are typically caused by the generation of oxygen species in the conversion from DOX to semiquinone, yielding very reactive hydroxyl radicals. The free radical may also cause damage to various membrane lipids and other cellular components [31]. Pathological examination 10 days following a single dose injection of doxorubicin revealed there were significant cardiac differences between the s.c. HA–DOX and i.v. DOX formulations. Of the animals that received i.v. DOX, 83% developed myocarditis and cardiac myocyte degeneration. Other significant lesions included thrombosis and muscle inflammation around the thrombus. In contrast, only 20% of animals that received s.c. HA–DOX developed very subtle myocyte degeneration. No lesions or inflammation were observed for 80% of the animals in the s.c. HA–DOX group, which clearly demonstrates that HA–DOX formulation greatly reduces the cardiac toxicity of doxorubicin in a rodent model. Furthermore, our pathology studies demonstrated that the skin and cutaneous tissues at the injection site were devoid of inflammation or necrosis both 6 and 24 h after HA–DOX injection. This finding may be corroborated clinically with the use of hyaluronan as a rescue medication to alleviate local toxicity effects of doxorubicin that has extravasated into the subcutaneous tissues following dislodgement of the i.v. catheter during intravenous administration. This effect was confirmed in tissue biopsies at the conclusion of the study (10 days post injection) which demonstrated no substantial damage to the underlying tissue at the injection site. Therefore, HA–DOX conjugates have potential to reduce the incidence of local skin and soft tissue toxicity from doxorubicin chemotherapy, which would improve patient tolerance and compliance in a clinical application.

Another strategy for reducing doxorubicin associated cardiac and liver toxicity is metronomic chemotherapy, which involves continuous administration of doxorubicin at regular short intervals as opposed to a bolus dosing with a higher concentration of the drug [32]. Metronomic dosing regimens decrease the non-specific toxicity of an anticancer drug in normal cells. In addition, in a study by Pastorino et al., a metronomic chemotherapy of NGR peptide coupled liposomal doxorubicin greatly hindered the progression of orthotopic neuroblastoma xenografts in an immunodeficient mouse model [33]. This dosing regimen however has its own drawbacks clinically in that more frequent intravenous doses are required which adds to patient discomfort, time spent in infusions, and creates nursing as well as compliance issues. HA–DOX by subcutaneous injection weekly would have great benefits over standard or metronomic dosing regimens both in terms of patient compliance and tolerance, but also with regard to potential improved toxicity and efficacy. Further translational efforts will focus on optimizing dose frequency and completing preclinical proof of concept.

Acknowledgments

This work was supported by awards from the National Institutes of Health (R21 CA132033 and P20 RR015563), the American Cancer Society (RSG-08-133-01-CDD), the Susan G. Komen Foundation (KG090481), and an Eli Lilly Predoctoral Fellowship to SC.

Appendix A. Supplementary data

Supplementary data associated with this article can be found, in the online version, at doi: 10.1016/j.jconrel.2010.04.006.

References

[1] G. Takemura, H. Fujiwara, Doxorubicin-induced cardiomyopathy from the cardiotoxic mechanisms to management, Prog. Cardiovasc. Dis. 49 (5) (2007) 330–352.
[2] Y. Matsumura, T. Hamaguchi, T. Ura, K. Muro, Y. Yamada, Y. Shimada, K. Shirao, T. Okusaka, H. Ueno, M. Ikeda, N. Watanabe, Phase I clinical trial and pharmacokinetic evaluation of NK911, a micelle-encapsulated doxorubicin, Br. J. Cancer 91 (10) (2004) 1775–1781.
[3] B. Rihova, J. Strohalm, J. Prausova, K. Kubackova, M. Jelinkova, L. Rozprimova, M. Sirova, D. Plocova, T. Etrych, V. Subr, T. Mrkvan, M. Kovar, K. Ulbrich, Cytostatic and immunomobilizing activities of polymer-bound drugs: experimental and first clinical data, J. Control. Release 91 (1–2) (2003) 1–16.
[4] A.W. Tolcher, S. Sugarman, K.A. Gelmon, R. Cohen, M. Saleh, C. Isaacs, L. Young, D. Healey, N. Onetto, W. Slichenmyer, Randomized phase II study of BR96-doxorubicin conjugate in patients with metastatic breast cancer, J. Clin. Oncol. 17 (2) (1999) 478–484.
[5] National Cancer Institute: Breast cancer PDQ treatment, 2007, <http://www.cancer.gov/cancertopics/pdq/treatment/breast/HealthProfessional> Access date 10/29/2009.
[6] P. Querzoli, M. Pedriali, R. Rinaldi, A.R. Lombardi, E. Biganzoli, P. Boracchi, S. Ferretti, C. Frasson, C. Zanella, S. Ghisellini, F. Ambrogi, L. Antolini, M. Piantelli, S. Iacobelli, E. Marubini, S. Alberti, I. Nenci, Axillary lymph node nanometastases are prognostic factors for disease-free survival and metastatic relapse in breast cancer patients, Clin. Cancer Res. 12 (22) (2006) 6696–6701.
[7] M.d. Boer, C.H.v. Deurzen, J.A.v. Dijck, G.F. Borm, P.J.v. Diest, E.M. Adang, J.W. Nortier, E.J. Rutgers, C. Seynaeve, M.B. Menke-Pluymers, P. Bult, V.C. Tjan-Heijnen, Micrometastases or isolated tumor cells and the outcome of breast cancer, N. Engl. J. Med. 361 (7) (2009) 653–663.
[8] J.R. Fraser, T.C. Laurent, Turnover and metabolism of hyaluronan, Ciba Found. Symp. 143 (1989) 41–53 discussion 53–49, 281–285.
[9] T. Ahrens, V. Assmann, C. Fieber, C. Termeer, P. Herrlich, M. Hofmann, J.C. Simon, CD44 is the principal mediator of hyaluronic-acid-induced melanoma cell proliferation, J. Invest. Dermatol. 116 (1) (2001) 93–101.
[10] A. Dietrich, E. Tanczos, W. Vanscheidt, E. Schopf, J.C. Simon, High CD44 surface expression on primary tumours of malignant melanoma correlates with increased metastatic risk and reduced survival, Eur. J. Cancer 33 (6) (1997) 926–930.
[11] M. Gotte, G.W. Yip, Heparanase, hyaluronan, and CD44 in cancers: a breast carcinoma perspective, Cancer Res. 66 (21) (2006) 10233–10237.

[12] S. Misra, S. Ghatak, B.P. Toole, Regulation of MDR1 expression and drug resistance by a positive feedback loop involving hyaluronan, phosphoinositide 3-kinase, and ErbB2, J. Biol. Chem. 280 (21) (2005) 20310–20315.
[13] A. Bartolazzi, R. Peach, A. Aruffo, I. Stamenkovic, Interaction between CD44 and hyaluronate is directly implicated in the regulation of tumor development, J. Exp. Med. 180 (1) (1994) 53–66.
[14] T. Asplund, P. Heldin, Hyaluronan receptors are expressed on human malignant mesothelioma cells but not on normal mesothelial cells, Cancer Res. 54 (16) (1994) 4516–4523.
[15] S. Sugahara, S. Okuno, T. Yano, H. Hamana, K. Inoue, Characteristics of tissue distribution of various polysaccharides as drug carriers: influences of molecular weight and anionic charge on tumor targeting, Biol. Pharm. Bull. 24 (5) (2001) 535–543.
[16] C. Cera, M. Palumbo, S. Stefanelli, M. Rassu, G. Palu, Water-soluble polysaccharide-anthracycline conjugates: biological activity, Anticancer Drug Des. 7 (2) (1992) 143–151.
[17] K. Akima, H. Ito, Y. Iwata, K. Matsuo, N. Watari, M. Yanagi, H. Hagi, K. Oshima, A. Yagita, Y. Atomi, I. Tatekawa, Evaluation of antitumor activities of hyaluronate binding antitumor drugs: synthesis, characterization and antitumor activity, J. Drug Target. 4 (1) (1996) 1–8.
[18] Y. Luo, G.D. Prestwich, Synthesis and selective cytotoxicity of a hyaluronic acid-antitumor bioconjugate, Bioconjug. Chem. 10 (5) (1999) 755–763.
[19] K.H. Bouhadir, E. Alsberg, D.J. Mooney, Hydrogels for combination delivery of antineoplastic agents, Biomaterials 22 (19) (2001) 2625–2633.
[20] X. Xu, R. Sutak, D.R. Richardson, Iron chelation by clinically relevant anthracyclines: alteration in expression of iron-regulated genes and atypical changes in intracellular iron distribution and trafficking, Mol. Pharmacol. 73 (3) (2008) 833–844.
[21] S. Cai, Y. Xie, T. Bagby, M.S. Cohen, M.L. Forrest, Intralymphatic chemotherapy using a hyaluronan-cisplatin conjugate, J. Surg. Res. 147 (2) (2008) 247–252.
[22] A.H.M.A.M. Al-Ghananeem, Y.M. Muammer, J.M. Balko, E.P. Black, W. Mourad, E. Romond, Intratumoral delivery of paclitaxel in solid tumor from biodegradable hyaluronan nanoparticle formulations, AAPS PharmSciTech 10 (2) (2009) 410–417.
[23] R.M.D. Peer, Loading mitomycin C inside long circulating hyaluronan targeted nano-liposomes increases its antitumor activity in three mice tumor models, Int. J. Cancer 108 (5) (2004) 780–789.
[24] A.K. Yadav, P. Mishra, A.K. Mishra, S. Jain, G.P. Agrawal, Development and characterization of hyaluronic acid-anchored PLGA nanoparticulate carriers of doxorubicin, Nanomedicine 3 (4) (2007) 246–257.
[25] A.K. Yadav, P. Mishra, S. Jain, A.K. Mishra, G.P. Agrawal, Preparation and characterization of HA-PEG-PCL intelligent core-corona nanoparticles for delivery of doxorubicin, J. Drug Target. 16 (6) (2008) 464–478.
[26] H. Lee, C.H. Ahn, T.G. Park, Poly[lactic-co-(glycolic acid)]-grafted hyaluronic acid copolymer micelle nanoparticles for target-specific delivery of doxorubicin, Macromol. Biosci. 9 (4) (2009) 336–342.
[27] R. Soloman, A.A. Gabizon, Clinical pharmacology of liposomal anthracyclines: focus on pegylated liposomal doxorubicin, Clin. Lymphoma Myeloma 8 (1) (2008) 21–32.
[28] D. Lorusso, A.D. Stefano, V. Carone, A. Fagotti, S. Pisconti, G. Scambia, Pegylated liposomal doxorubicin-related palmar-plantar erythrodysesthesia ('hand–foot' syndrome), Ann. Oncol. 18 (7) (2007) 1159–1164.
[29] M.E. O'Brien, N. Wigler, M. Inbar, R. Rosso, E. Grischke, A. Santoro, R. Catane, D.G. Kieback, P. Tomczak, S.P. Ackland, F. Orlandi, L. Mellars, L. Alland, C. Tendler, Reduced cardiotoxicity and comparable efficacy in a phase III trial of pegylated liposomal doxorubicin HCl (CAELYX/Doxil) versus conventional doxorubicin for first-line treatment of metastatic breast cancer, Ann. Oncol. 15 (3) (2004) 440–449.
[30] P.E. Wallemacq, A. Capron, R. Vanbinst, E. Boeckmans, J. Gillard, B. Favier, Permeability of 13 different gloves to 13 cytotoxic agents under controlled dynamic conditions, Am. J. Health Syst. Pharm. 63 (6) (2006) 547–556.
[31] R.D. Olson, P.S. Mushlin, Doxorubicin cardiotoxicity: analysis of prevailing hypotheses, FASEB J. 4 (13) (1990) 3076–3086.
[32] A.J. Quesada, T. Nelius, R. Yap, T.A. Zaichuk, A. Alfranca, S. Filleur, O.V. Volpert, J.M. Redondo, In vivo upregulation of CD95 and CD95L causes synergistic inhibition of angiogenesis by TSP1 peptide and metronomic doxorubicin treatment, Cell Death Differ. 12 (6) (2005) 649–658.
[33] F. Pastorino, C. Brignole, D. Marimpietri, M. Cilli, C. Gambini, D. Ribatti, R. Longhi, T.M. Allen, A. Corti, M. Ponzoni, Vascular damage and anti-angiogenic effects of tumor vessel-targeted liposomal chemotherapy, Cancer Res. 63 (21) (2003) 7400–7409.